Supporting Information For:

In Situ Catalyst Generation and Benchtop-Compatible Entry Points for Ti^{II}/Ti^{IV} Redox Catalytic Reactions

Zachary W. Davis-Gilbert,[a] Kento Kawakita,[b] Daniel C. Blechschmidt,[a] Hayato Tsurugi,[b]* Kazushi Mashima,[b]* and Ian A. Tonks[a]*

[a]Department of Chemistry, University of Minnesota – Twin Cities, Minneapolis, MN 55455

[b]Department of Chemistry, Graduate School of Engineering Science, Osaka University, Toyonaka, Osaka 560-8531, Japan

Solvent Scope for the formation of 3a

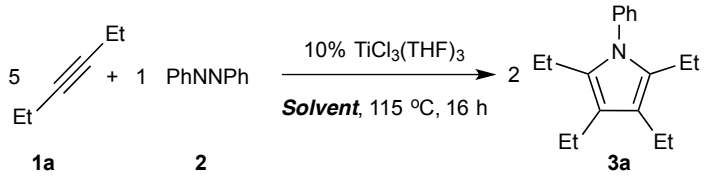

^{1}H NMR (400 MHz, C_6H_5Br) δ, ppm: 2.40 (q, J = 7.5 Hz, 4H), 2.28 (q, J = 7.5 Hz, 4H), 1.10 (t, J = 7.5 Hz, 6H), 0.74 (t, J = 7.5 Hz, 6H).

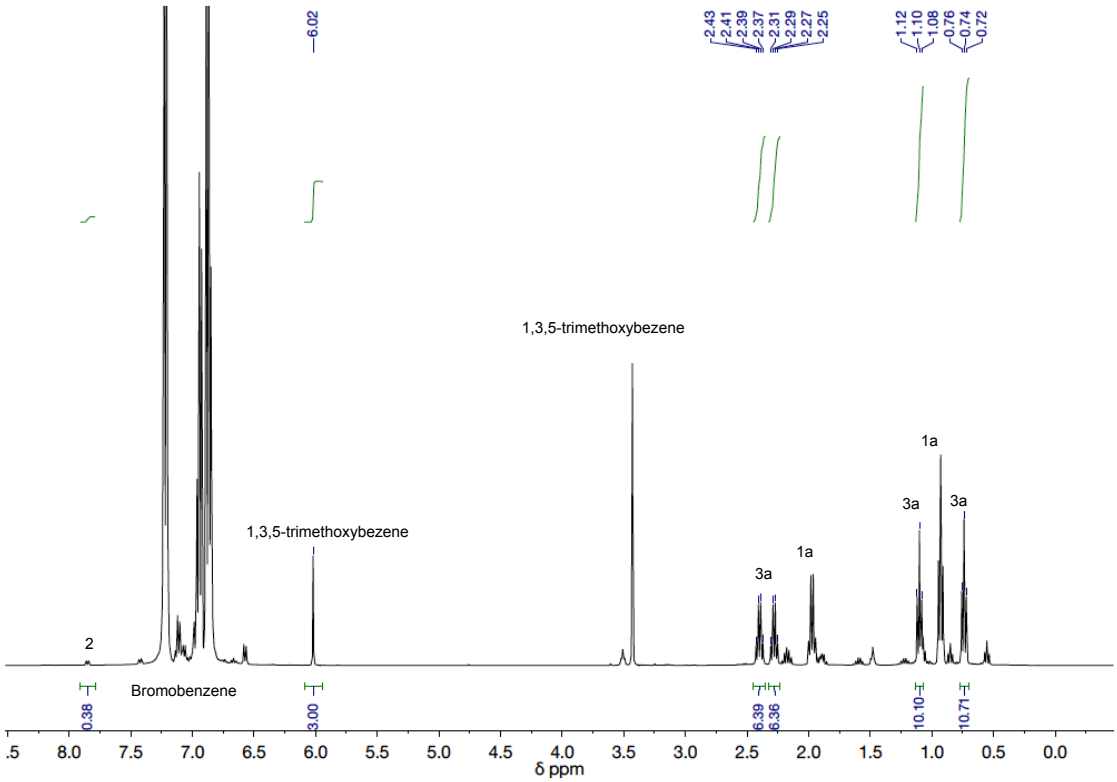

Figure S1. ^{1}H No-D NMR spectrum of the formation of **3a** in bromobenzene

^{1}H NMR (400 MHz, $C_6H_5CH_3$) δ, ppm: 2.44 (q, J = 7.5 Hz, 4H), 2.30 (q, J = 7.4 Hz, 4H), 1.15 (t, J = 7.5 Hz, 6H), 0.77 (t, J = 7.5 Hz, 6H).

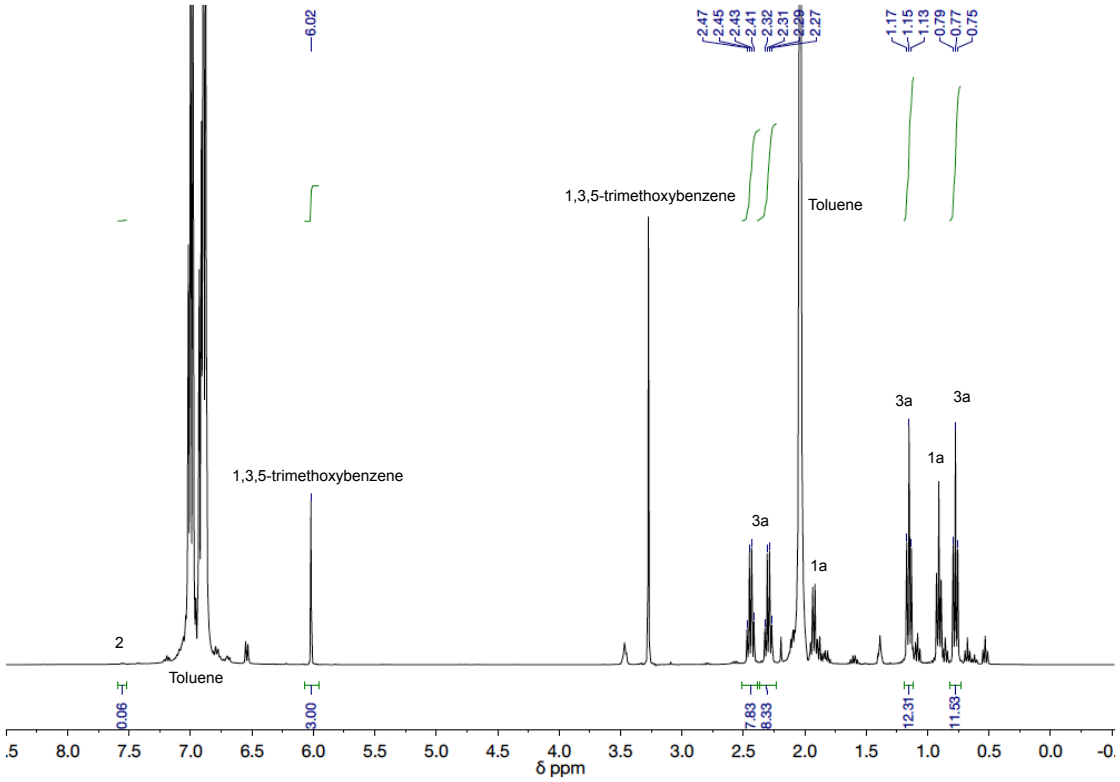

Figure S2. ^{1}H No-D NMR spectrum of the formation of **3a** in toluene.

^{1}H NMR (400 MHz, $C_6H_5OCH_3$) δ, ppm: 2.39 (q, J = 7.5 Hz, 4H), 2.26 (q, J = 7.5 Hz, 4H), 1.09 (t, J = 7.5 Hz, 6H), 0.73 (t, J = 7.5 Hz, 6H).

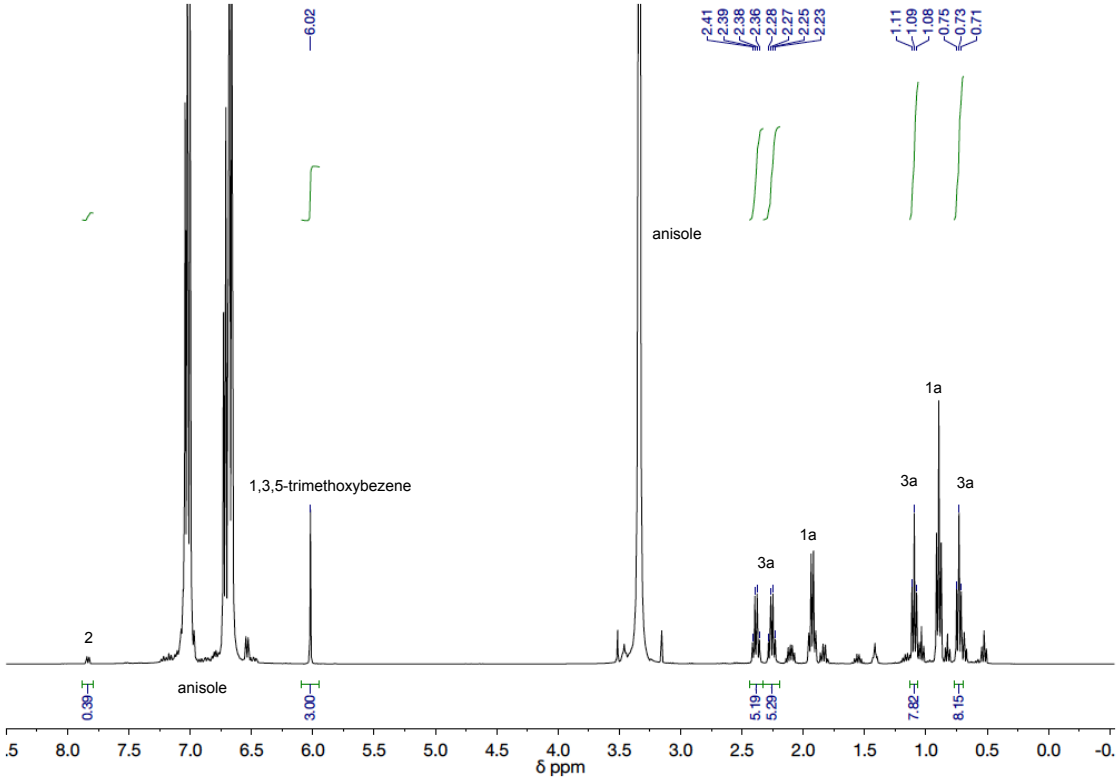

Figure S3. ^{1}H No-D NMR spectrum of the formation of **3a** in anisole.

^{1}H NMR (400 MHz, $C_6H_5CF_3$) δ, ppm: 2.41 (q, J = 7.5 Hz, 4H), 2.28 (q, J = 7.5 Hz, 4H), 1.09 (t, J = 7.5 Hz, 6H), 0.72 (t, J = 7.5 Hz, 6H).

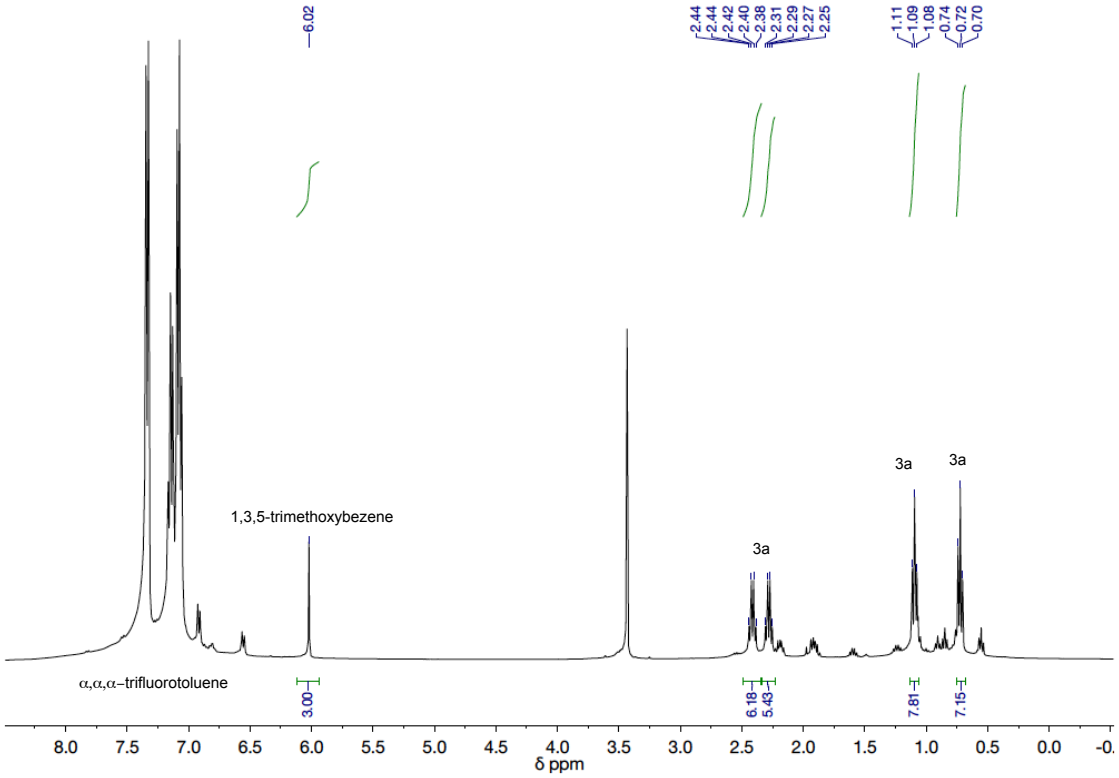

Figure S4. ^{1}H No-D NMR spectrum of the formation of 3a in α,α,α-trifluorotoluene.

^{1}H NMR (400 MHz, *o*-$C_6H_4Cl_2$) δ, ppm: 2.43 (q, *J* = 7.6 Hz, 4H), 2.33 (q, *J* = 7.5 Hz, 4H), 1.13 (t, *J* = 7.4 Hz, 6H), 0.78 (t, *J* = 7.4 Hz, 6H).

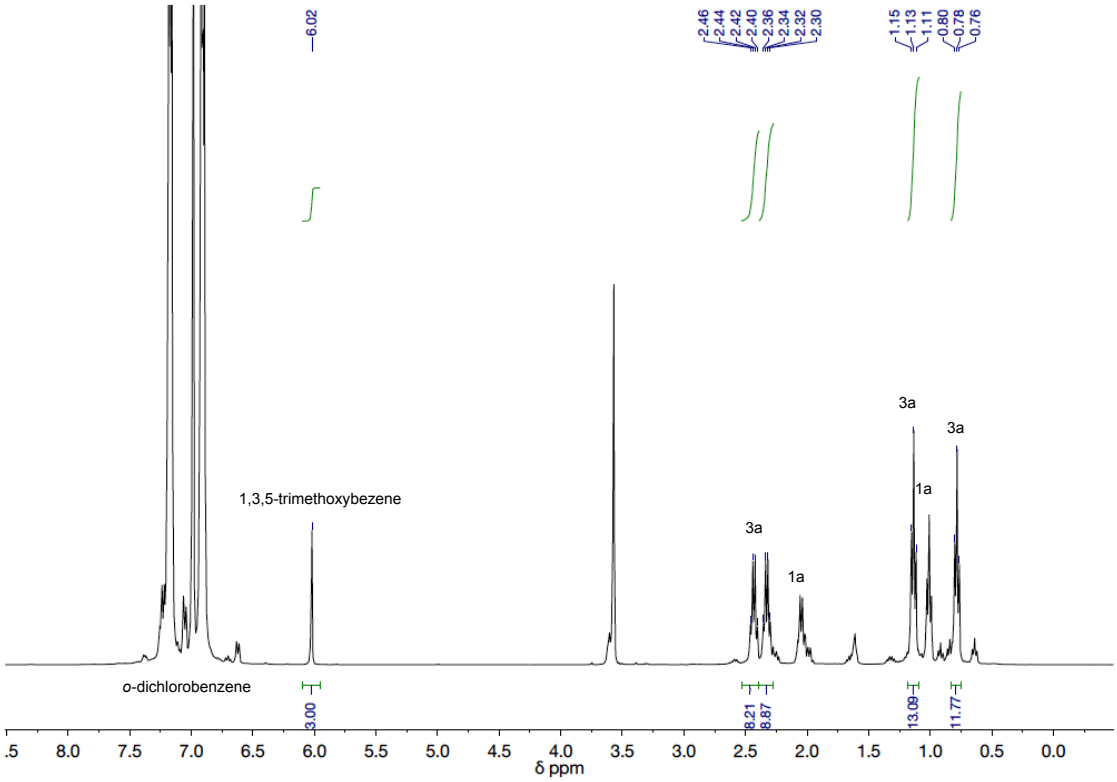

Figure S5. ^{1}H No-D NMR spectrum of the formation of **3a** in *o*-dichlorobenzene.

Zn^0 Optimization

Table S1 Zn^0 optimization for the reduction of $TiCl_4THF_2$ in the [2+2+1] pyrrole formation.[a]

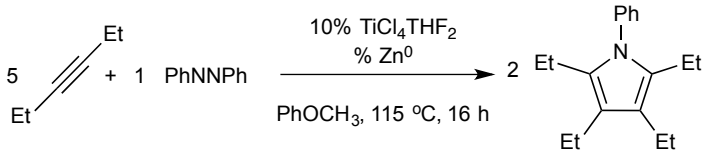

mol % Zn^0	NMR Yield (%)
10	94
10[b]	99
10[c]	0
20	90
40	90

[a]Conditions: 0.19 mmol azobenzene, 0.96 mmol 3-hexyne, 0.019 mmol $TiCl_4THF_2$, 0.1 mmol trimethoxybenzene (TMB) as internal standard and using >15 year old Zn^0 powder (FischerChemical, Lot No. 028036) in 0.5 mL of $PhOCH_3$ at 115 °C. [b]New Zn^0 powder. [c]Granular 20-30 mesh Zn^0 SigmaAldrich.

Independent Synthesis of [Ti(NPh)Cl$_2$(4-picoline)$_3$] (4)

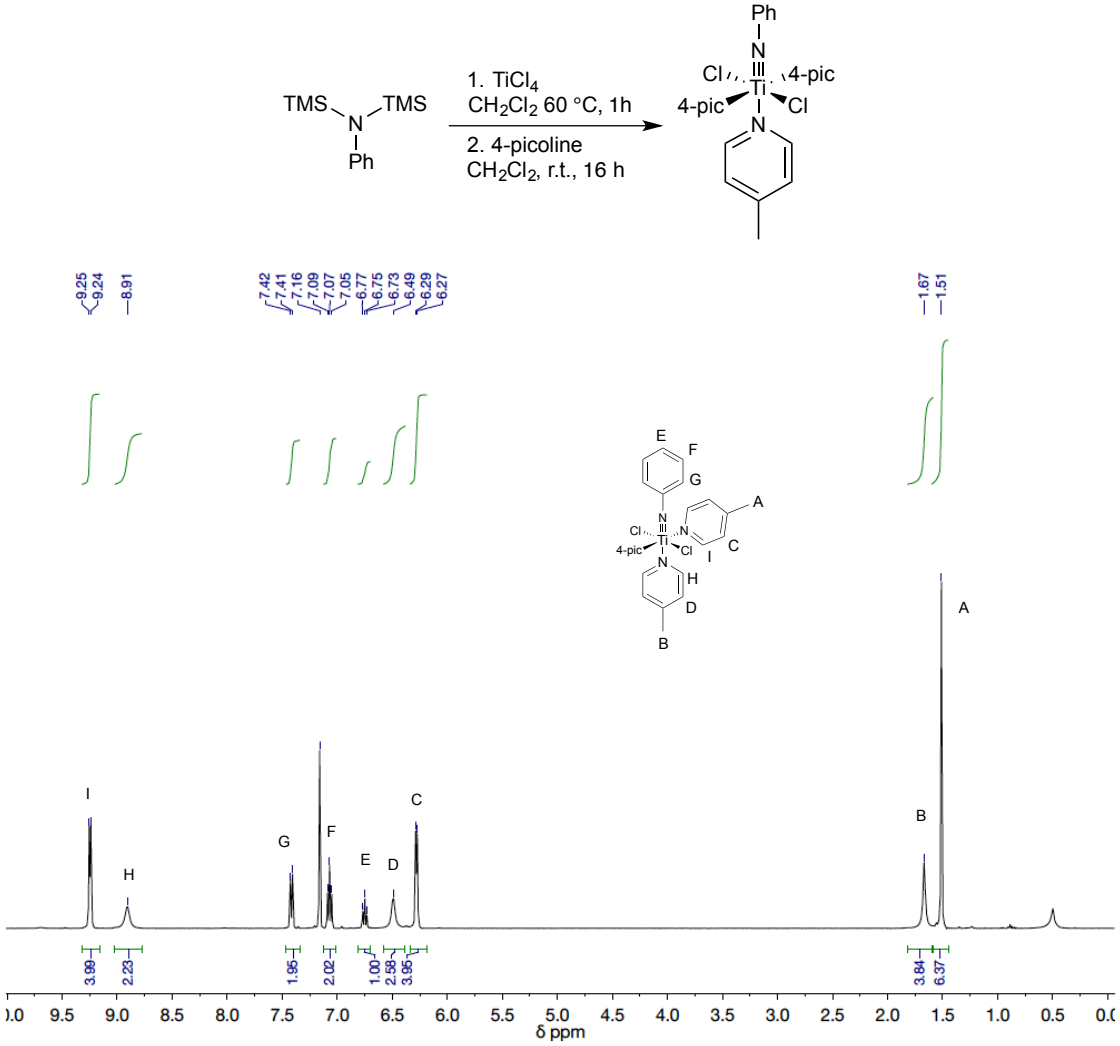

Figure S6. ^{1}H NMR spectrum of **[Ti(NPh)Cl$_2$(4-picoline)$_3$] (4)** in C_6D_6.

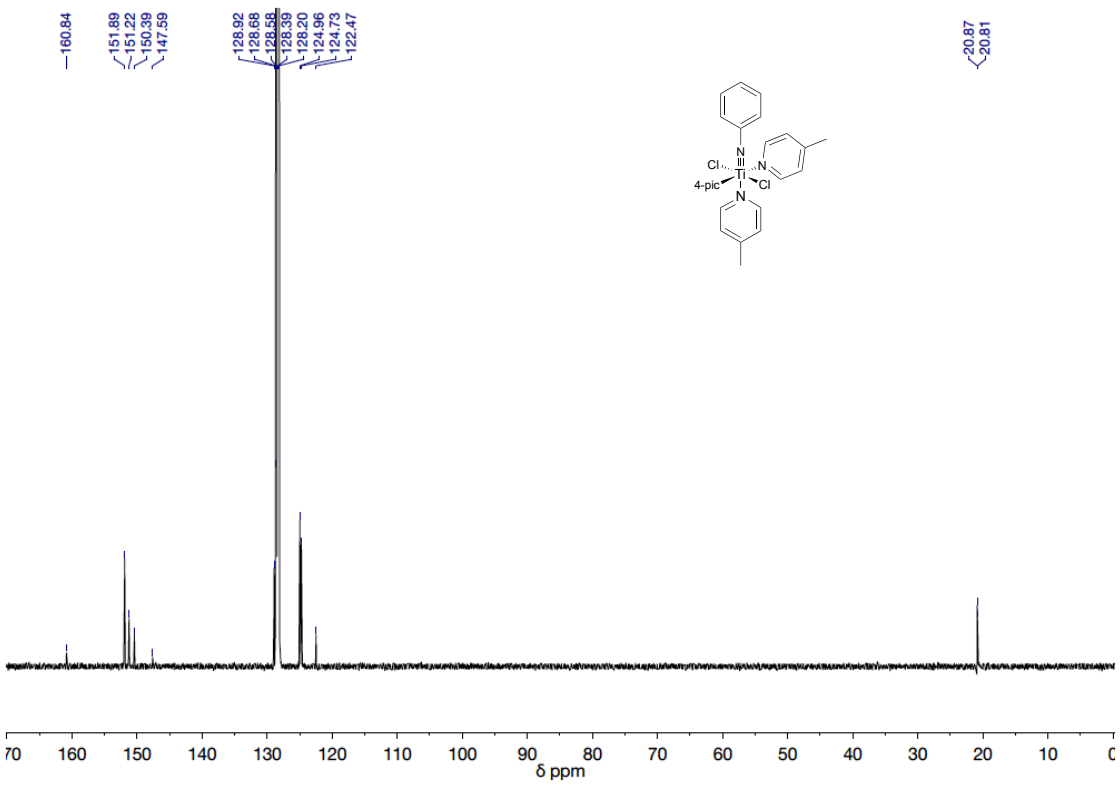

Figure S7. ^{13}C NMR spectrum of **[Ti(NPh)Cl$_2$(4-picoline)$_3$] (4)** in C_6D_6.

NMR Reaction for the formation of 3a

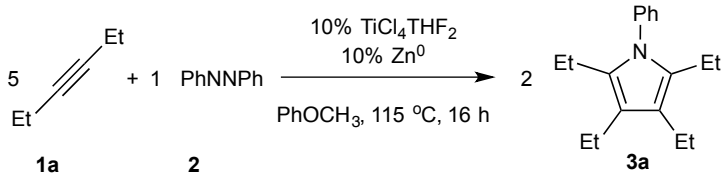

^{1}H NMR (500 MHz, $C_6H_5OCH_3$) δ, ppm: 2.39 (q, *J* = 7.5 Hz, 4H), 2.26 (q, *J* = 7.5 Hz, 4H), 1.10 (t, *J* = 7.5 Hz, 6H), 0.73 (t, *J* = 7.5 Hz, 6H).

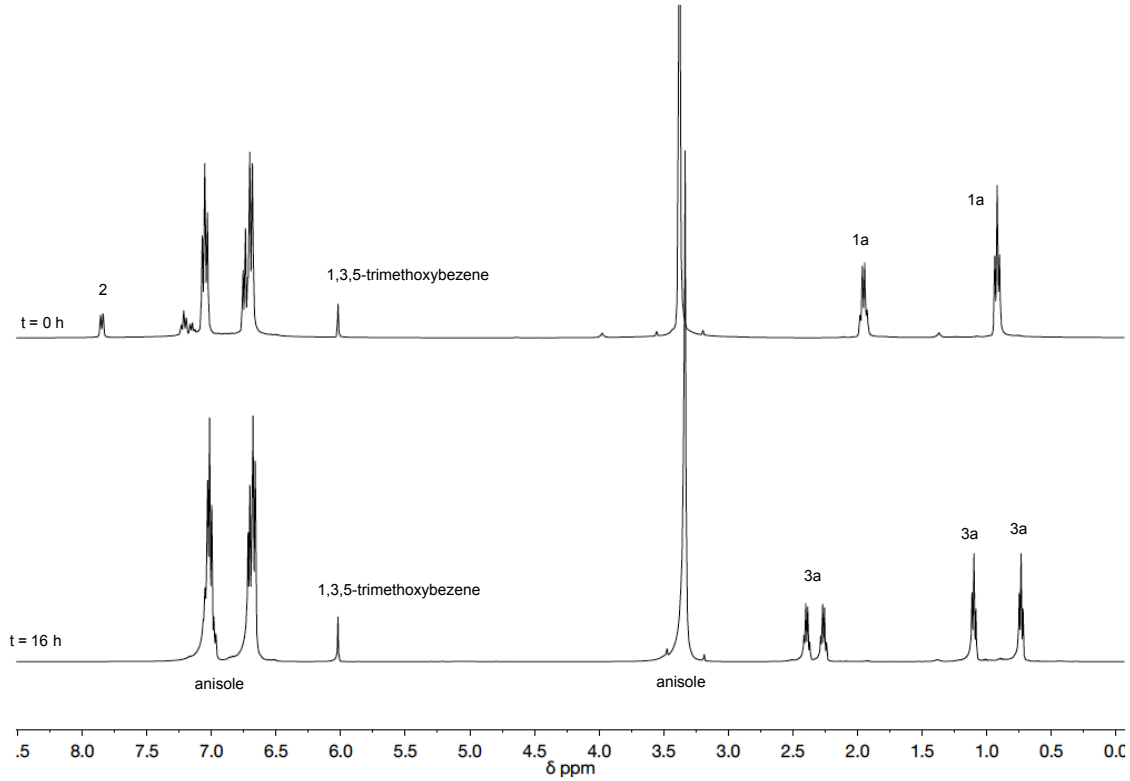

Figure S8. ^{1}H No-D NMR spectrum at t = 0 h (top) and t =16 h (bottom) of the formation of **3a** in anisole.

NMR Reaction for the formation of 3b

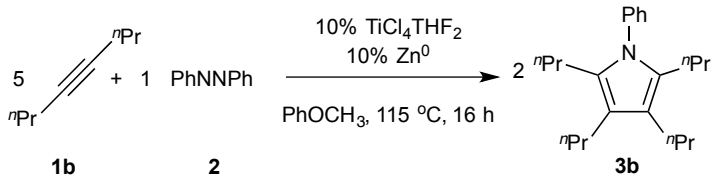

1b **2** **3b**

^{1}H NMR (400 MHz, $C_6H_5OCH_3$) δ, ppm: 2.51 – 2.34 (m, 4H, -C*H*$_2$CH$_2$CH$_3$), 2.35 – 2.13 (m, 4H, -C*H*$_2$CH$_2$CH$_3$), 1.62 – 1.46 (m, 4H, -CH$_2$C*H*$_2$CH$_3$), 1.15 (h, *J* = 7.4 Hz, 4H, -CH$_2$C*H*$_2$CH$_3$), 0.91 (t, *J* = 7.4 Hz, 6H, -CH$_2$CH$_2$C*H*$_3$), 0.58 (t, *J* = 7.4 Hz, 6H, -CH$_2$CH$_2$C*H*$_3$).

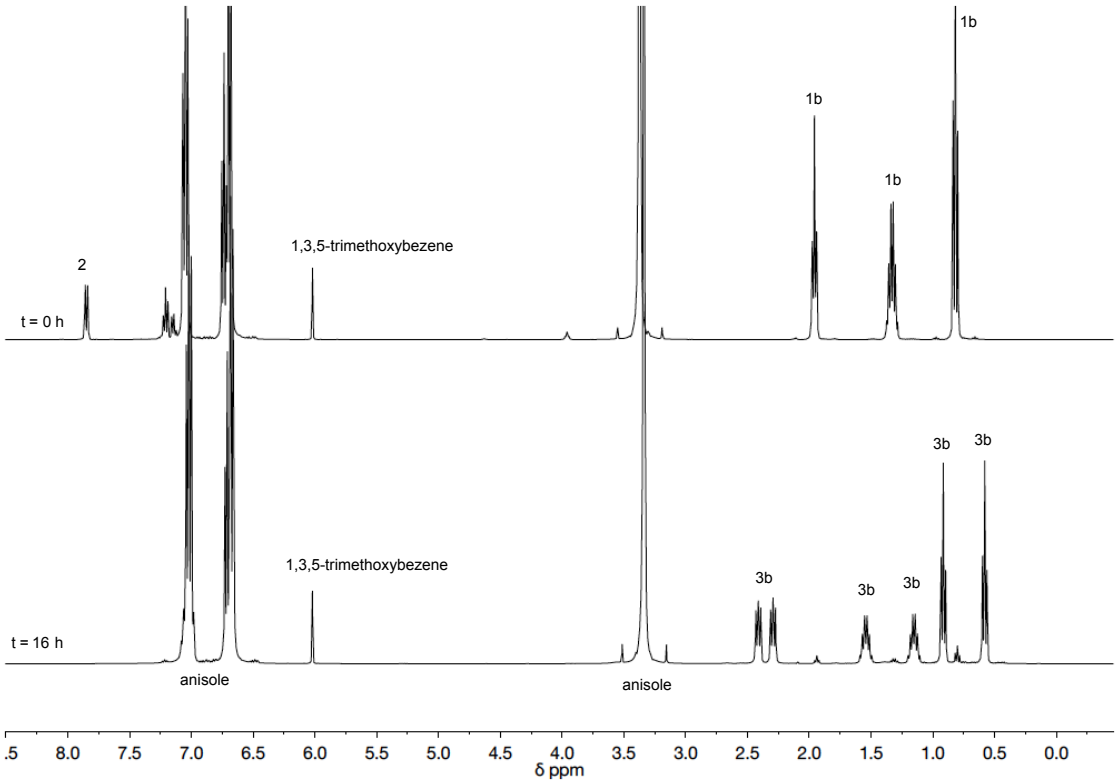

Figure S9. ^{1}H No-D NMR spectrum at t = 0 h (top) and t =16 h (bottom) of the formation of **3b** in anisole.

NMR Reaction for the formation of 3ca-cc

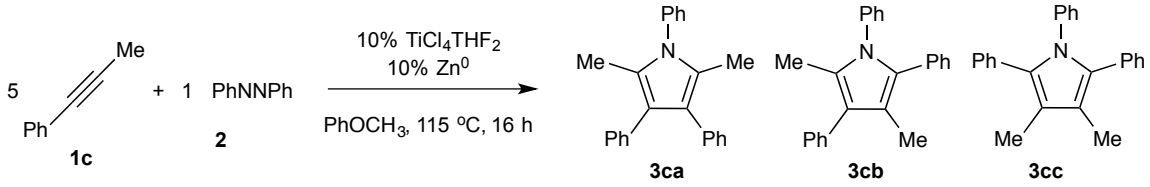

3ca

^{1}H NMR (400 MHz, $C_6H_5OCH_3$) δ, ppm: 1.91 (s, 6H, 2,5-pyrrole-(CH_3)$_2$)

3cb

^{1}H NMR (400 MHz, $C_6H_5OCH_3$) δ, ppm: 2.09 (s, 3H, 2-pyrrole-CH_3), 1.95 (s, 3H, 4-pyrrole-CH_3)

3cc

^{1}H NMR (400 MHz, $C_6H_5OCH_3$) δ, ppm: 1.98 (s, 3H, 3,4-pyrrole-(CH_3)), 1.86 (s, 3H, 3,4-pyrrole-(CH_3)).

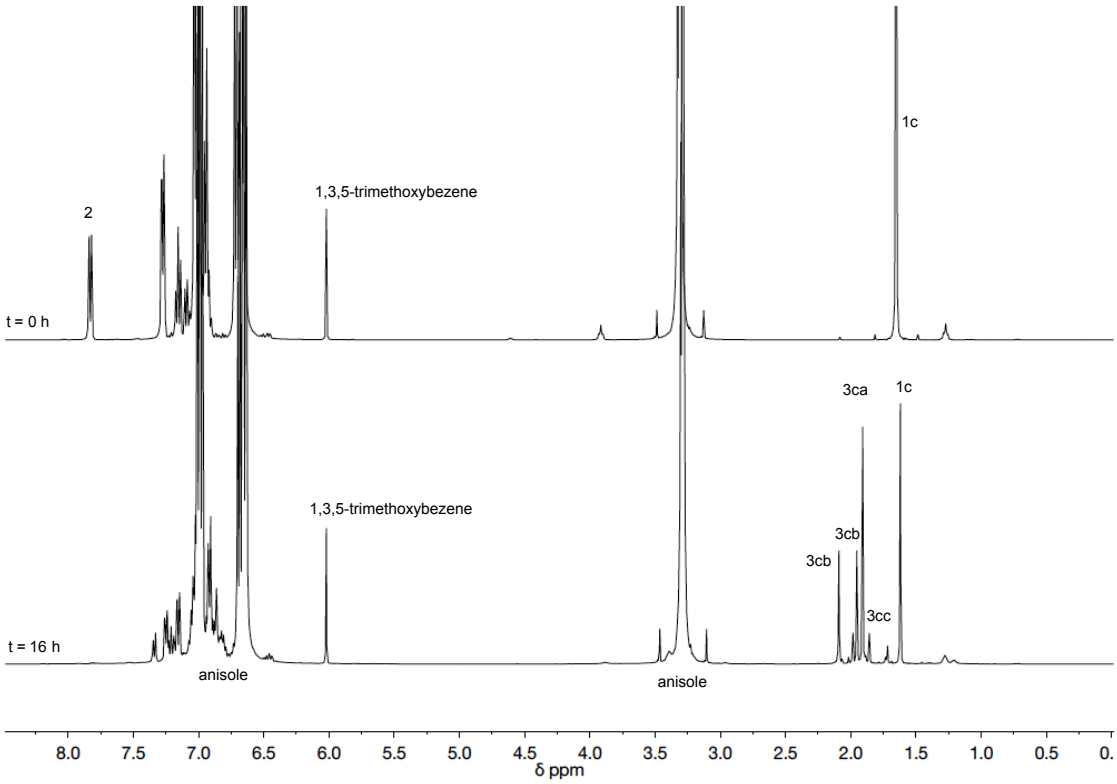

Figure S10. ^{1}H No-D NMR spectrum at t = 0 h (top) and t =16 h (bottom) of the formation of **3ca-c** in anisole.

NMR Reaction for the formation of 3d

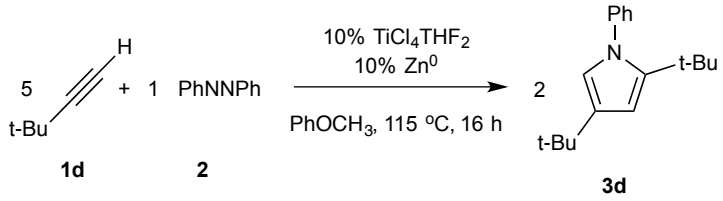

Due to overlap with TMB 5-bromo-m-xylene was used as internal standard. Referenced to 3.34 for anisole -OCH_3.
^{1}H NMR (400 MHz, $C_6H_5OCH_3$) δ, ppm: 6.26 (d, *J* = 2.1 Hz, 2H, Pyrrole-C*H*), 6.03 (d, *J* = 2.2 Hz, 2H, Pyrrole-C*H*), 1.22 (s, 9H, Pyrrole-C(C*H*$_3$)$_3$), 1.05 (s, 9H, Pyrrole-C(C*H*$_3$)$_3$).

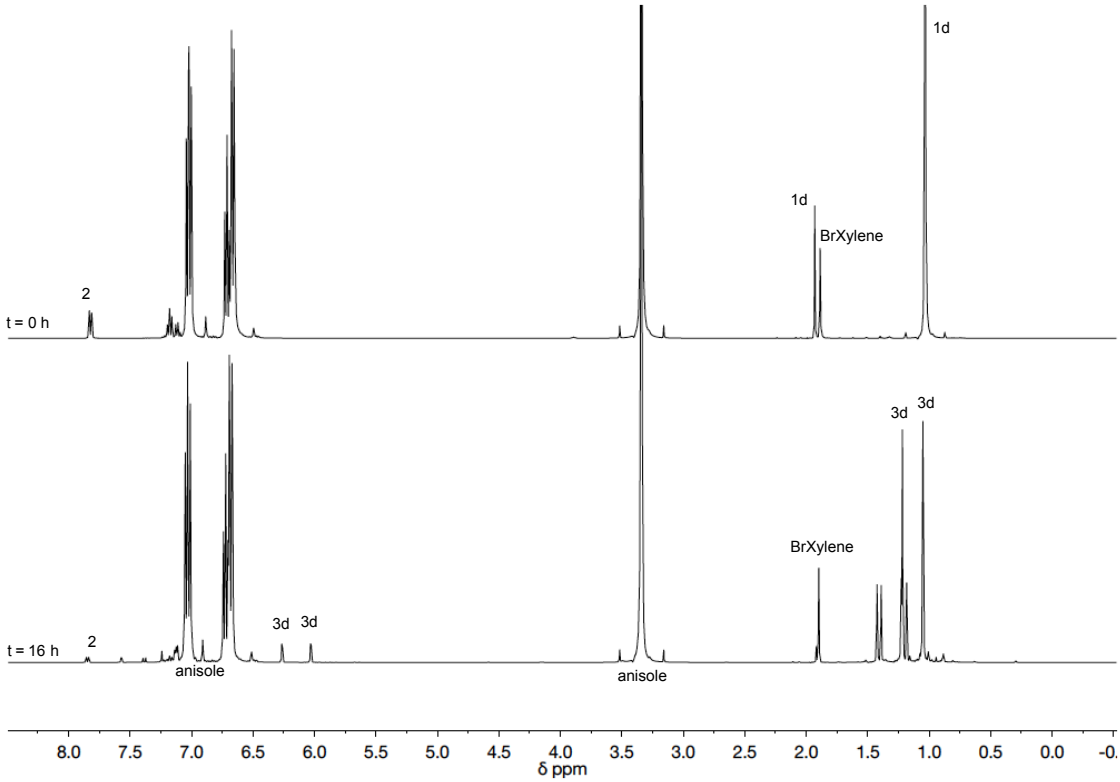

Figure S11. ^{1}H No-D NMR spectrum at t = 0 h (top) and t =16 h (bottom) of the formation of **3d** in anisole.

NMR Reaction for the formation of 3e

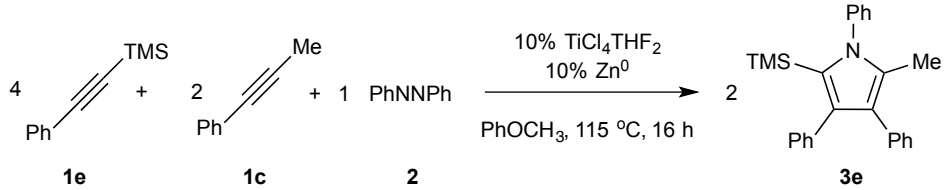

1e **1c** **2** **3e**

^{1}H NMR (400 MHz, $C_6H_5OCH_3$) δ, ppm: 7.33 – 7.20 (m, 5H, -C_6H_5), 1.91 (s, 3H, PyrroleCH_3), -0.31 (s, 9H, PyrroleSi(CH_3)$_3$).

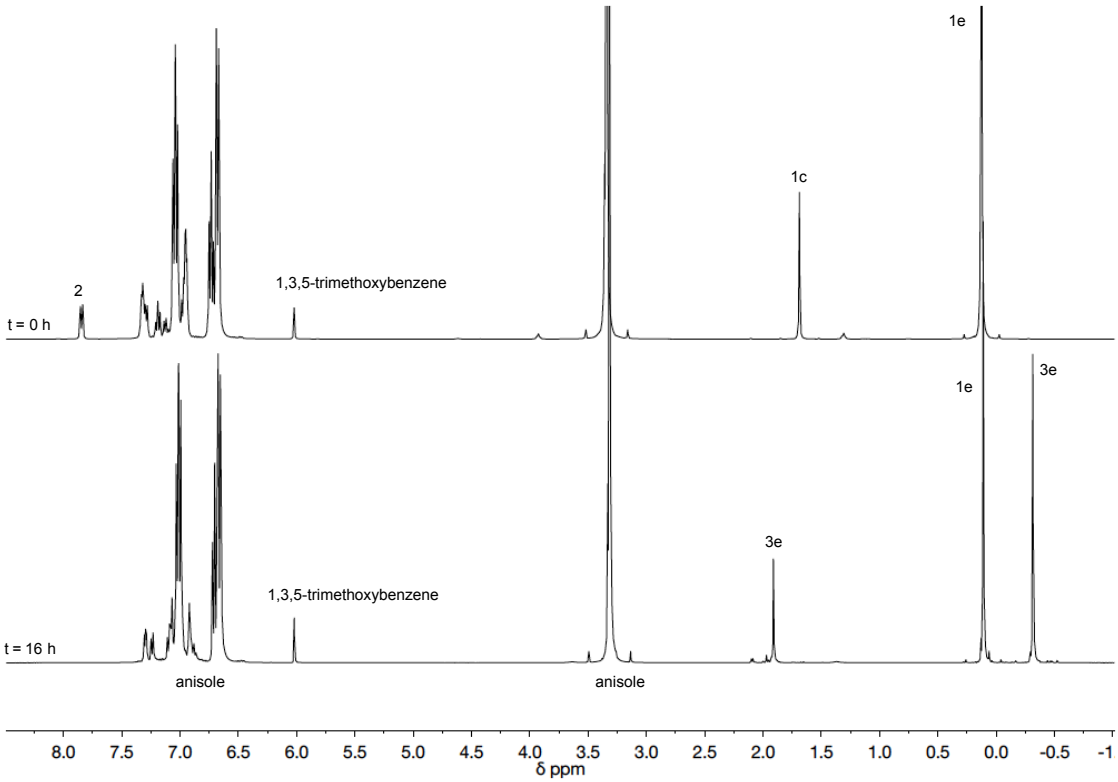

Figure S12. ^{1}H No-D NMR spectrum at t = 0 h (top) and t =16 h (bottom) of the formation of **3e** in anisole.

NMR Reaction for the formation of 3f

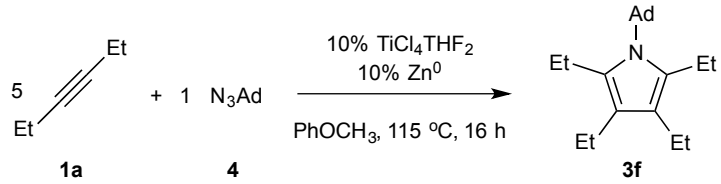

1a **4** **3f**

^{1}H NMR (400 MHz, $C_6H_5OCH_3$) δ, ppm: 2.72 (q, *J* = 7.2 Hz, 4H, -C*H*$_2$CH$_3$), 2.31 (q, *J* = 7.5 Hz, 4H, -C*H*$_2$CH$_3$), 2.19 (d, *J* = 3.0 Hz, 6H, N-C-(C*H*$_3$)$_3$), 1.91 (br s, 3H, Ad-methine), 1.56 – 1.43 (m, 6H, Ad), 1.06 (m, 12H, -CH$_2$C*H*$_3$).

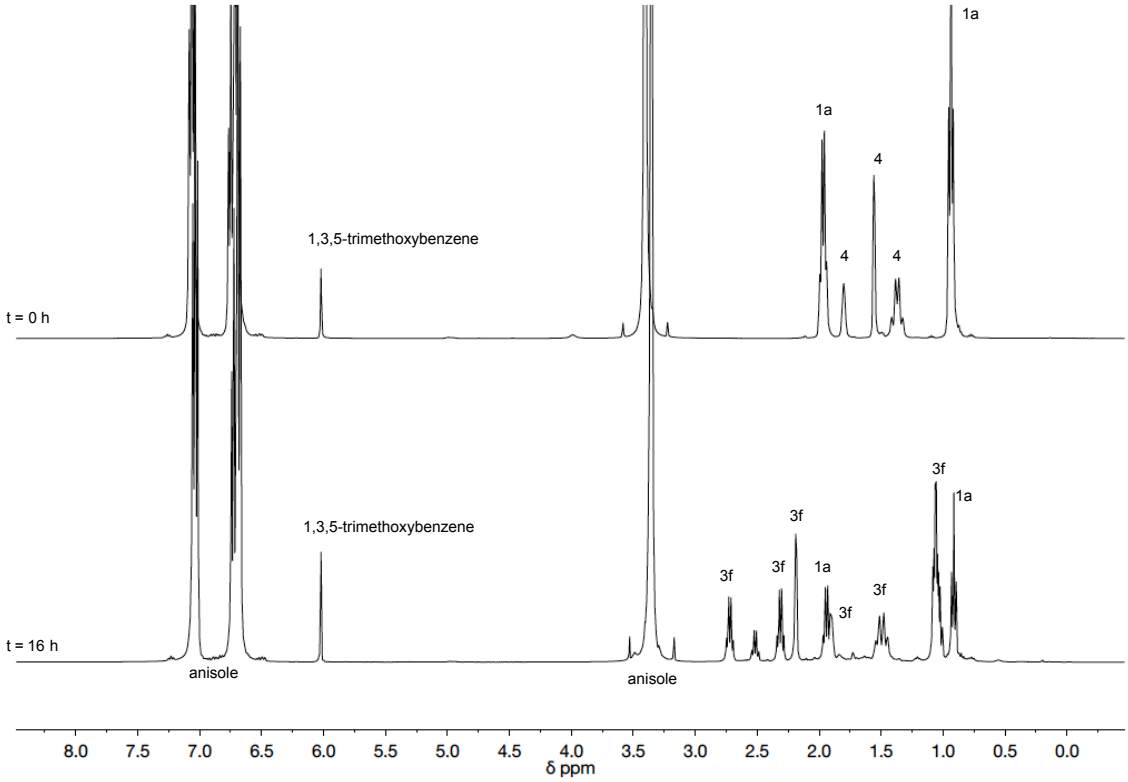

Figure S13. ^{1}H No-D NMR spectrum at t = 0 h (top) and t =16 h (bottom) of the formation of **3f** in anisole.

NMR Reaction for the formation of 3g

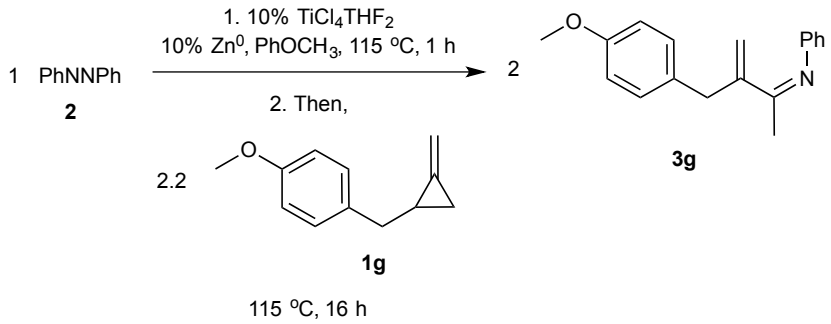

^{1}H NMR (400 MHz, $C_6H_5OCH_3$) δ, ppm: 5.41 (s, 1H, -C=CH*H*), 5.19 (s, 1H -C=CH*H*), 3.72 (s, 2H, -ArC*H*$_2$C=C-), 1.62 (s, 3H C(=NPh)CH_3).

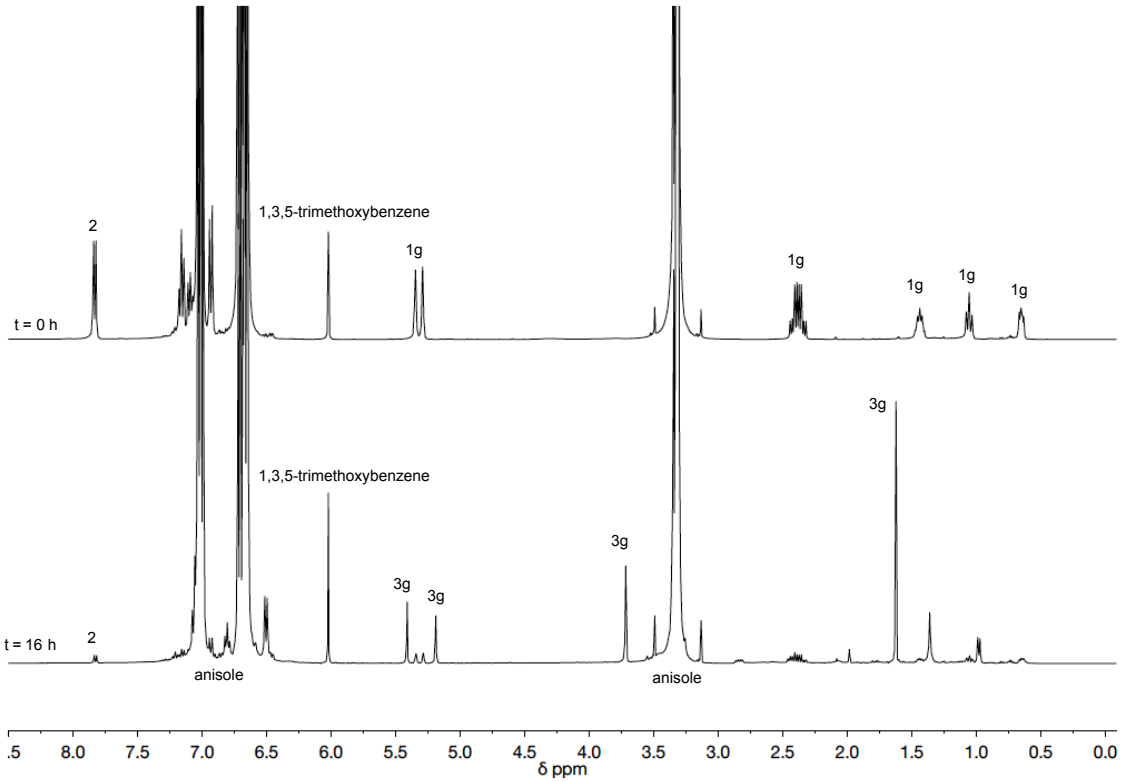

Figure S14. ^{1}H No-D NMR spectrum at t = 0 h (top) and t =16 h (bottom) **3g** in anisole.

NMR Reaction for the formation of 3h

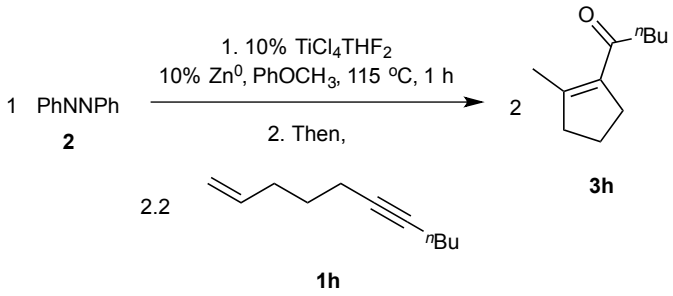

^{1}H NMR (400 MHz,$C_6H_5OCH_3$) δ, ppm: 2.33 (m, 2H, -C=CCH_2CH$_2$-), 2.14 (t, J = 7.3 Hz, 2H, -C(O)CH_2CH$_2$-), 2.07 (td, J = 7.9, 3.2 Hz, 2H, -C=CCH_2CH$_2$-), 1.86 (s, 3H, C=CCH_3), 1.57 – 1.37 (m, 4H, -CH$_2$CH_2CH$_2$-), 1.13 (sext, J = 7.3 Hz, 2H, -CH$_2$CH_2CH$_3$), 0.74 (t, J = 7.3 Hz, 3H, -CH$_2$CH$_2$CH_3).

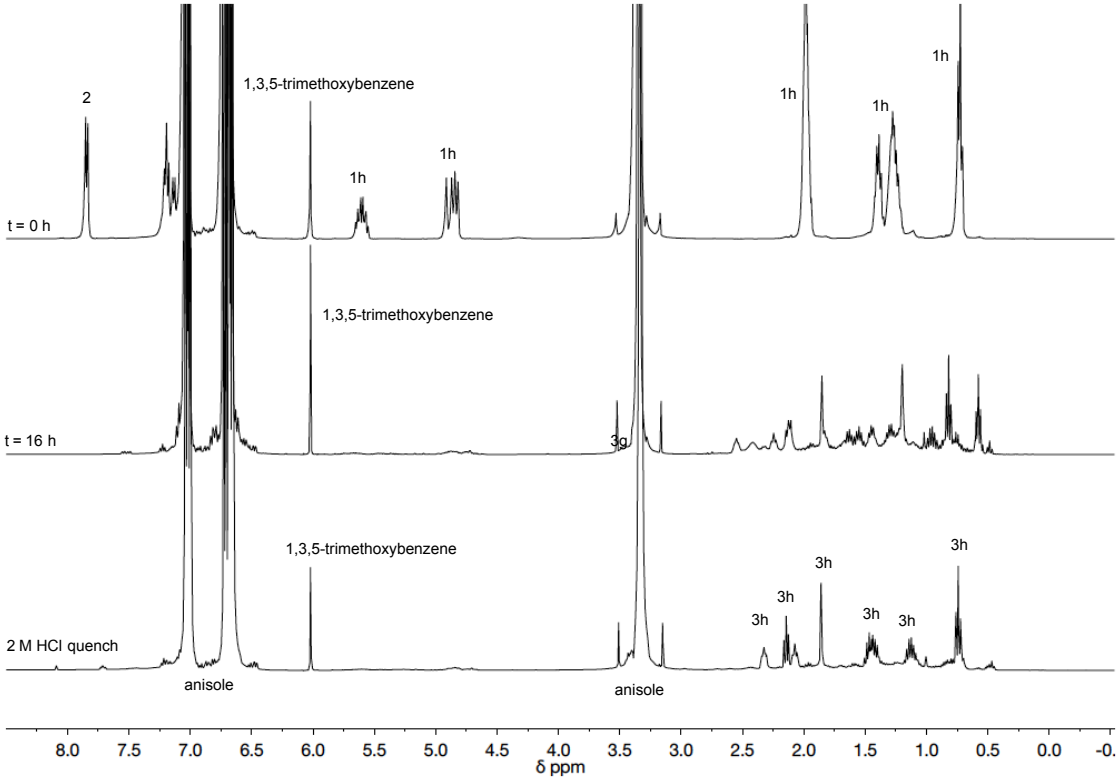

Figure S15. ^{1}H No-D NMR spectrum at t = 0 h (top), t =16 h (middle), t = 16 h (2M HCl quench, bottom) of the formation of **3h** in anisole.

NMR Reaction for the formation of 3i

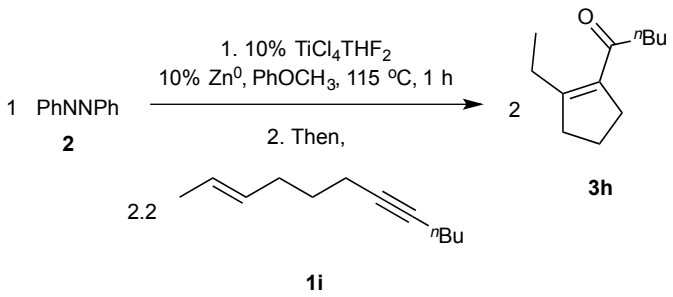

^{1}H NMR (400 MHz, $C_6H_5OCH_3$) δ, ppm: 2.41 (q, J = 7.6 Hz, 2H, -C=CCH_2CH$_3$), 2.31 (t, J = 7.7 Hz, 2H, , -C=CCH_2CH$_2$-), 2.20 – 2.06 (m, 4H), 1.59 – 1.34 (m, 4H, , -CH$_2$CH_2CH$_2$-), 1.12 (h, J = 7.5 Hz, 2H, -CH$_2$CH_2CH$_3$), 0.86 (t, J = 7.5 Hz, 3H, -CCH$_2$CH_3), 0.73 (t, J = 7.3 Hz, 3H, -CH$_2$CH$_2$CH_3).

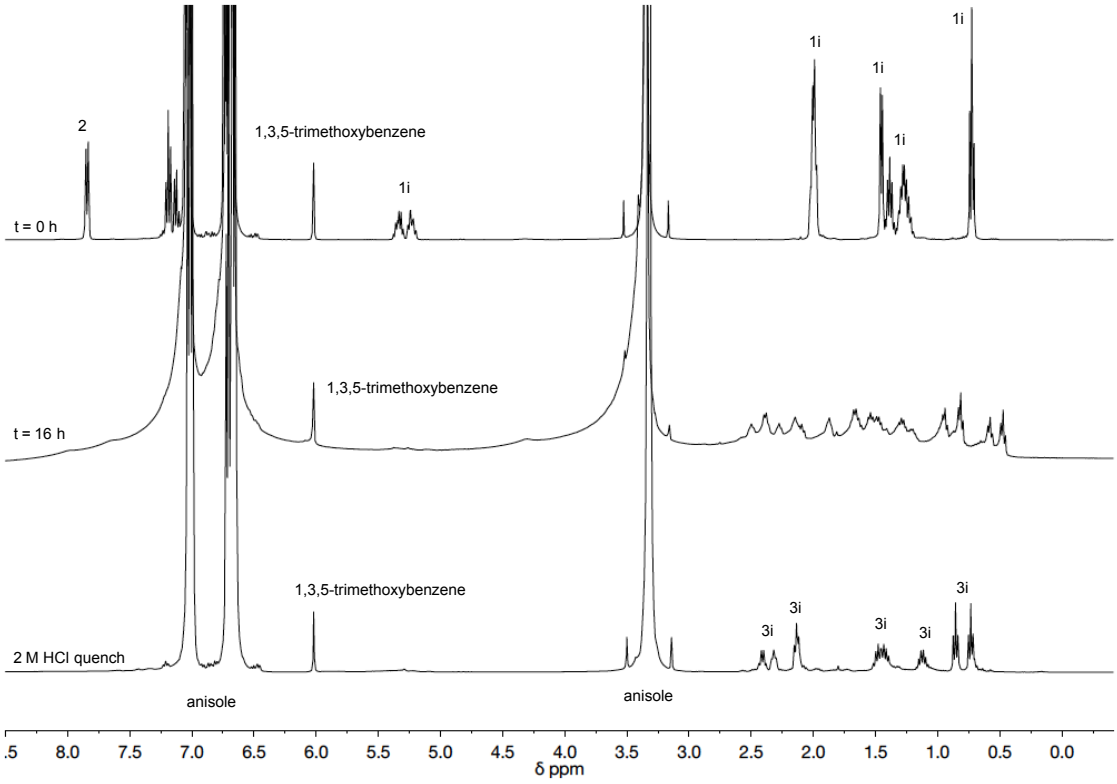

Figure S16. ^{1}H No-D NMR spectrum at t = 0 h (top), t =16 h (middle), t = 16 h (2M HCl quench, bottom) of the formation of **3i** in anisole.

NMR Reaction for the formation of 3j

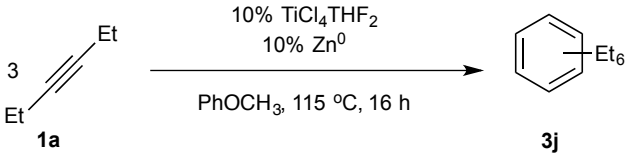

^{1}H NMR (400 MHz, $C_6H_5OCH_3$) δ, ppm: 2.51 (q, J = 7.5 Hz, 12H, $C_6(CH_2CH_3)_6$), 1.01 (t, J = 7.4 Hz, 18H, $C_6(CH_2CH_3)_6$).

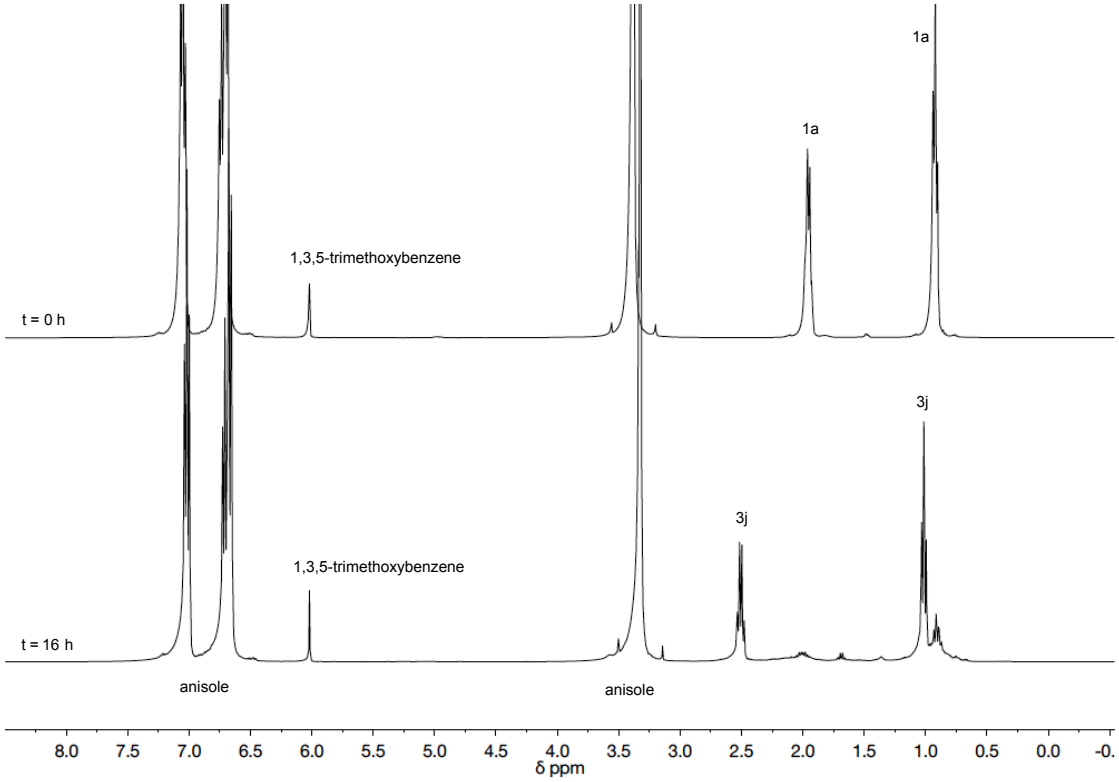

Figure S17. ^{1}H No-D NMR spectrum at t = 0 h (top) and t =16 h (bottom) of the formation of **3j** in anisole.

Scale up bench top reaction for the formation of 3a

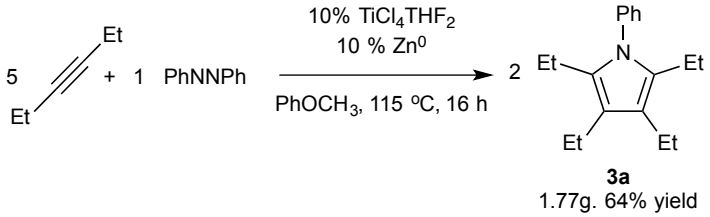

3a
1.77g. 64% yield

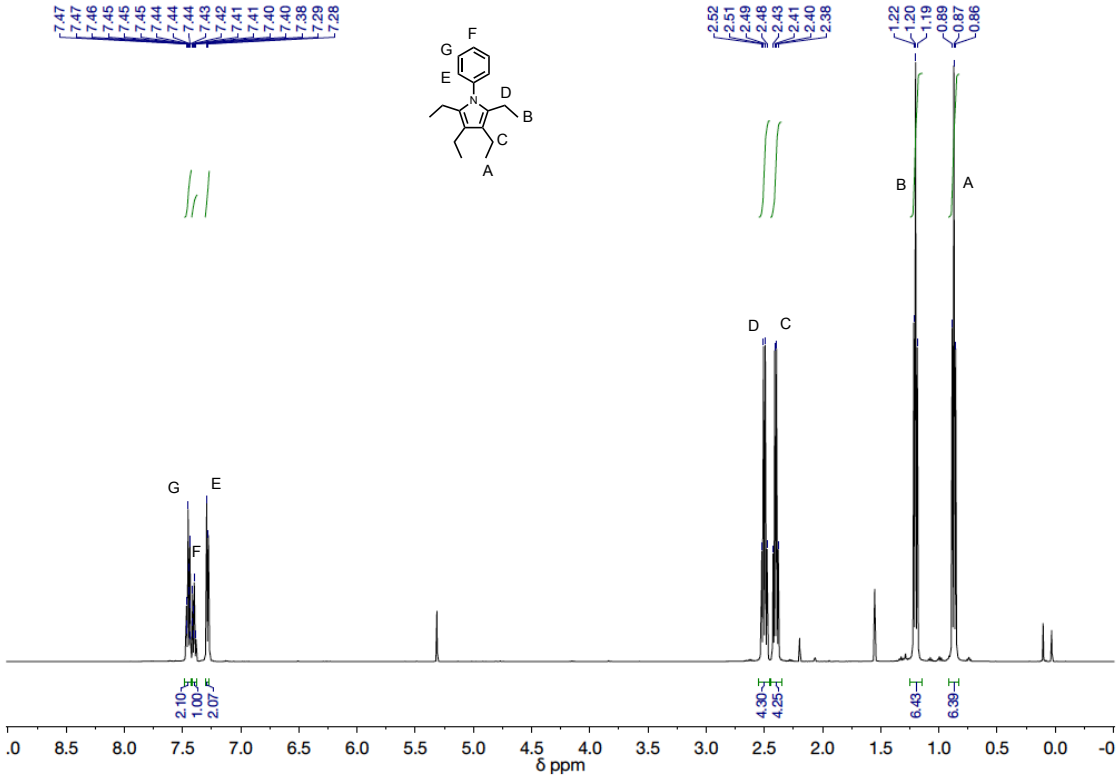

Figure S18. ^{1}H NMR Spectrum of **3a** in $CDCl_3$